Overlap Concentration Generates Optimum Device Performance For DPP-based Conjugated Polymers

Rahul Venkatesh,[‡] Yulong Zheng,[†] Aaron L. Liu,[‡] Haoqun Zhao,[‡] Carlos Silva,[†,§,||] Christopher J. Takacs,[#] Martha Grover,[‡,*] Carson Meredith[‡,*], and Elsa Reichmanis[¶,*]

[‡]*School of Chemical and Biomolecular Engineering, Georgia Institute of Technology, 311 Ferst Drive NW, Atlanta GA 30332, United States*

[†]*School of Chemistry and Biochemistry, Georgia Institute of Technology, 901 Atlantic Drive, Atlanta GA 30332, United States*

[§]*School of Physics, Georgia Institute of Technology, 837 State Street, Atlanta GA 30332, United States*

[||]*School of Materials Science and Engineering, Georgia Institute of Technology, 771 Ferst Drive NW, Atlanta GA 30332, United States*

[#] *Stanford Synchrotron Radiation Light Source, SLAC National Accelerator Laboratory, Menlo Park, CA 94025, United States*

[¶]*Department of Chemical & Biomolecular Engineering, Lehigh University, 124 E. Morton Street, Bethlehem PA 18015, United States*

E-mail: elr420@lehigh.edu; martha.grover@chbe.gatech.edu; carson.meredith@chbe.gatech.edu

Abstract

Manipulating the solution phase of conjugated polymers via control of the respective processing parameters results in opportunities to create new morphologies and function. Although the complex processing space of conjugated polymers has been widely investigated, the effect of polymer solution concentration has not been adequately linked to macroscale device performance. This work investigates the influence of the processing parameter, solution concentration, on the OFET performance of donor-acceptor polymers, with a focus on diketopyrrolopyrrole (DPP)-based polymers using solution viscosity experiments. Experiments performed on three different molecular weights (M_w) of poly[2,5-(2-octyldodecyl)-3,6-diketopyrrolopyrrole-alt-5,5-(2,5-di(thien-2-yl)thieno- [3,2-b]-thiophene)] (DPP-DTT) revealed that films fabricated at the critical overlap concentration (C*), identified from solution-state viscosity experiments, consistently resulted in improved organic field effect transistor hole mobility. The overlap of polymer chains at C* in the solution state is shown to be related to formation of ordered morphologies that may explain the improved charge transport in the solid film. Furthermore, similar experiments revealed that the trend is observed across other types of DPP-based polymers as well.

Keywords

Diketopyrrolopyrrole (DPP), conjugated polymer, donor-acceptor polymer, solution concentration, critical overlap concentration, entanglement, solution-phase, organic field effect transistor.

INTRODUCTION

Push-pull copolymers, commonly referred to as donor-acceptor (D-A) polymers, are garnering increasing attention as promising alternatives to traditional inorganic semiconductors for the production of cost-efficient, printable, deformable, and large-area electronic devices such as organic light emitting diodes (OLEDs),[1] organic photovoltaics (OPVs),[2] organic field effect transistors (OFETs),[3, 4] and biomedical sensors.[5] D-A polymers are particularly attractive alternatives to their homopolymer counterparts such as poly(3-hexylthiophene) (P3HT) and exhibit improved electronic performance due to their rigid, planar backbone conformation with minimal steric hindrance between the donor and acceptor units.[6, 7] As with homopolymer semiconductors, the ability to process D-A polymers from solution provides process-oriented degrees of freedom and is expected to decrease the energy footprint associated with device fabrication.[8, 9]

In addition to intrinsic polymer properties such as the monomer chemical structure[10-14] and molecular weight,[7, 15] research on conjugated polymers has identified the impact of processing conditions such as solvent quality,[16-18] blend composition,[19, 20] dissolution temperature,[21, 22] coating speed,[23, 24] and annealing temperature[25] on final film morphology, which ultimately influences device performance. Unlike P3HT, where substantial research has led to OFET device mobilities reaching up to 1 $cm^2/V{\cdot}s$,[26] significant knowledge gaps exist in the process-structure-property (PSP) relationships of D-A polymers, creating room for discovery and vastly superior performance attributes.[6] To exploit the full potential of D-A polymers, a detailed investigation of the solution state in conjunction with thin-film characterization is required to obtain understanding of the phenomena that influence and control polymer chain conformation and aggregation, final film morphology, and device performance.[16, 18, 27-29] Disregarding solution state behavior can lead to imperfect understanding of critical PSP relationships and subsequently the final thin-film properties.[27]

A common strategy to manipulate the solution behavior of conjugated polymers to achieve desired thin-film morphology and improved device performance is to tune solvent quality[16-18, 28] or control

solution temperature,[21, 22] but other strategies have also been explored. Previous work by our group identified the significant influence of the processing variable, solution concentration, on the optoelectronic properties of poly[2,5-(2-octyldodecyl)-3,6-diketopyrrolopyrrole-alt-5,5-(2,5-di(thien-2-yl)thieno-[3,2-b]-thiophene)] (DPP-DTT).[30] Interestingly, it was observed that OFET devices prepared from the critical overlap concentration (C*) resulted in improved device performance and thin films prepared at semi-dilute concentrations displayed more interchain (H-aggregate) behavior. Although previous studies have tuned the solution concentration to induce aggregation[31, 32], to the best of our knowledge, the effect of concentration has not been adequately linked to macroscale device performance of D-A polymers and this relationship is yet to be fully understood. Investigating the solution phase will allow us to better understand the transitions taking place from the solution state to the final thin film.

Solution viscosity provides information on the behavior of polymer chains in solution and has been used effectively to probe polymer-solvent interactions, chain conformations, and degree of entanglements of well-known flexible polymers; their solution phase conformations and dynamics are generally well understood.[33, 34] However, the behavior of conjugated polymers in solution differs from that of flexible polymers due to their more rigid, semiflexible backbones with more anisotropic geometries and conjugated backbone interactions, which makes their aggregate structure and chain conformation more difficult to predict using previously developed models.[16, 35, 36] While a few studies on semiconducting polymers such as P3HT point to solution viscosity as an indicator of polymer solution behavior and its impact on solidified thin-film charge transport,[37] [15] to the best of our knowledge, the chain overlap concentration is not a factor that has been considered to explain the solution state behavior of D-A polymers or its impact on resultant film morphology and charge transport characteristics.

In this work, using DPP-DTT as a model for other DPP-based candidates, we study the influence of solution concentration on the polymer charge transport characteristics as determined by OFET device performance. The concentration dependence of DPP-DTT, at different molecular weights, was interrogated in both the solution state and thin films. Photophysical, morphological and electronic performance was explored using UV-Vis absorption spectroscopy, atomic force microscopy (AFM), grazing incidence wide angle X-ray (GIWAXS) scattering experiments and OFET device performance. The results were correlated with solution concentration. Notably,

similar results were observed for another DPP based polymer; poly[2,5-bis(2-octyldodecyl)pyrrolo[3,4-c]pyrrole-1,4(2H,5H)-dione-3,6-diyl)-alt-(2,2';5',2'';5'',2'''-quaterthiophen-5,5'''-diyl)] (PDPP-4T) suggesting that the observed phenomenon may be applicable to other DPP-based polymers as well.

MATERIALS AND METHODS

Sample Preparation: DPP-DTT at three different molecular weights (Batch M317: M_w = 290 kg mol^{-1} and PDI = 2.03, Batch M0311A2: M_w = 204 kg mol^{-1} and PDI = 3.09, Batch M0311A3: 110 kg mol^{-1} and PDI = 2.47) and PDPP-4T (Batch M0331A2: M_w = 75 kg mol^{-1} and PDI = 1.75) were purchased from Ossila Ltd. In order to determine the molecular weights of the samples, gel chromatography (GPC) was conducted by Ossila and the results are available on their website and the conditions for the GPC are discussed as follows. An Agilent PLgel Mixed C (300 x 7mm) x 2 was used as the column set. 1,2,4-Tricholorobenzene at 140 °C was used as a mobile phase at a flow rate of 1 mL/min. Polystyrene and toluene are used as the standard and flow rate marker respectively.

For DPP-DTT and PDPP-4T sample preparation, a stock solution was prepared by dissolving the polymer in chlorobenzene (anhydrous, Sigma-Aldrich) at 100 °C for 4 h, followed by continued heating at 56 °C overnight. The concentration of the stock solutions used for the respective polymers is shown in **Table S1** and the smaller concentrations were prepared from the respective stock solution. The thin films were prepared by blade coating the solutions onto the substrates (glass and OTS-18 treated silicon/SiO_2) at coating temperature of 56 °C, with a shearing speed of 2 mm/s followed by annealing at the same temperature for 10 min.

OFET Fabrication and Characterization: The OFET devices were prepared using heavily n-doped silicon substrates with a thermally grown SiO_2 dielectric layer and a bottom gate bottom contact configuration. A detailed description of the OFET fabrication and characterization process is provided in the supporting information of previously published results.[30]

Solution State Viscosity Measurement: Solution viscosity was measured using a DV2T Brookfield cone and plate viscometer with a CPA-40Z spindle. For DPP-DTT and PDPP-4T

solutions dissolved in chlorobenzene at different concentrations, the solution viscosity was measured at 56 °C using a setup consisting of a Brookfield TC-650 water bath.

Absorption Spectroscopy: Steady-state linear absorption measurements were performed using a Cary 5000 UV−Vis−NIR spectrometer on the solid thin-films deposited on glass substrates.

Atomic Force Microscopy: AFM images of the conjugated polymer thin films at varying solution concentrations deposited on glass substrates were obtained using tapping mode on a Bruker-Dimension ICON using HQ:NSC14/No Al (160 kHz, 5.0 N/m) tips purchased from MicroMasch.

Profilometry: Thickness of the DPP-DTT thin films on glass substrates was obtained using a Bruker DekakXT profilometer.

Cross Polarized Optical Microscopy: Optical Microscopy images of the conjugated polymer thin films at varying solution concentrations deposited on glass substrates were obtained using an Olympus BX51 microscope.

Grazing Incidence Wide-Angle X-ray Scattering (GIWAXS): GIWAXS measurements were conducted at the SLAC National Accelerator Laboratory on beamline SSRL 11-3. The beam was fixed at an energy of 12.7 keV and the critical angle was 0.12°. Conjugated polymer thin films of varying concentrations were prepared on bare silicon substrates using the same deposition and annealing technique mentioned above.

RESULTS

The impact of solution concentration on the optoelectronic properties of D-A polymers was investigated using DPP-DTT dissolved in chlorobenzene as a model (**Figure 1a**). Three different molecular weight samples were selected, namely DPP-DTT having a weight-average molecular weight (M_w) of 290 kg/mol, 204 kg/mol and 110 kg/mol. Solutions at different concentrations ranging from 1-12 g/L were prepared from concentrated stock solutions (**Table S1)**.

(a)

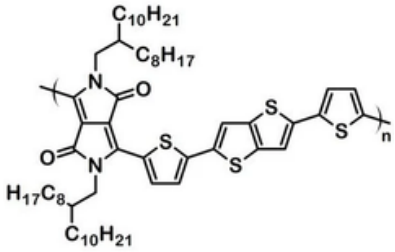

(b)

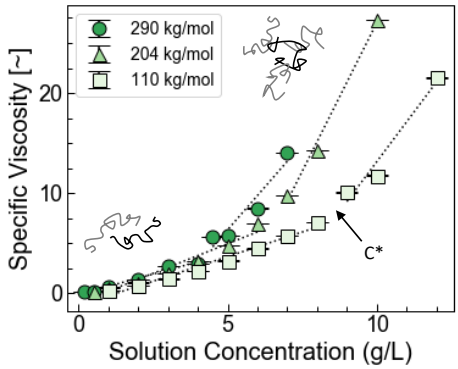

(c)

M_w (kg/mol)	C* (g/L)
290	4.5
204	6.5
110	8.5

(d)

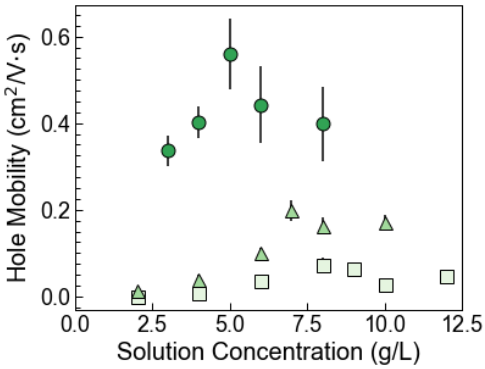

Figure 1. (a) Schematic of molecular structure of DPP-DTT. (b) Specific viscosity measurement of DPP-DTT at three molecular weights (290,[30] 204 and 110 kg/mol) dissolved in chlorobenzene solutions at 56 °C. The viscosity-concentration plot for 290 kg/mol DPP-DTT was adapted with permission from reference 30. Copyright 2021 American Chemical Society. The error bars represent the standard deviation of the specific viscosity. The schematic within the plot illustrates the extended, isolated polymer chains at dilute concentrations and overlapped polymer chains at semi-dilute concentrations. (c) The critical overlap concentration, C, values extracted from the viscosity-concentration plots for the three different molecular weights of DPP-DTT investigated. C* is the concentration at which the slopes of the two dashed lines intersect. (d) FET hole mobility of DPP-DTT thin films at three molecular weights (290,[30] 204 and 110 kg/mol) extracted from the backward sweep transfer curve (V_{DS} = -80V) as a function of solution concentration. The hole mobility-concentration plot for 290 kg/mol DPP-DTT was adapted with permission from reference 30. Copyright 2021 American Chemical Society. The error bars here represent 95% confidence intervals averaged over 18 OFET devices.*

Viscosity measurements of DPP-DTT:chlorobenzene solutions at different concentrations were performed to investigate the effect of solution concentration on the behavior of polymer chains in the solution state. An increase in the specific viscosity with increasing solution concentration for all three M_w's of DPP-DTT was observed (**Figure 1b**). Each sample exhibited two-regime behavior, with a power law slope increase in the specific viscosity occurring at the corresponding concentrations in **Figure 1c**. Similar behavior has been observed previously for linear polymer systems and the concentration at which the slope of the viscosity-concentration line changes is referred to as the critical overlap concentration (C*).[38-42] The C* values extracted from the viscosity-concentration plots for the three different molecular weights of DPP-DTT investigated are shown in the table in **Figure 1c**. Changes in the slope of the viscosity-concentration line for

the three M_w's investigated is provided in **Figure S1** and is in agreement with literature values.[38, 43, 44] C* typically indicates the transition from a dilute to a semi-dilute regime. In the dilute regime, it is believed that the polymer chains are separated from each other and behave independently. In the semi-dilute region, excess polymer chains may act as 'cross linkers' and begin to overlap, eventually resulting in entangled structures at high enough concentrations, thus explaining the significant increase in viscosity.[45] Furthermore, solutions at concentrations of C* and higher tend to form a gel upon aging for one week at room temperature as seen in **Figure S2**, while dilute solutions(<C*) at room temperature remain liquid irrespective of the aging time.

It is expected that C* increases as polymer M_w decreases: at a lower M_w the shorter polymer chains would require a greater solution concentration for the chains to interact and entangle[44]. In addition to experimental determination of C*, a theoretical value was calculated using the Huggins and Kramer equations (**Figure S3**).[33, 34, 46] While there is a significant difference between the experimental and theoretical values, the overall inverse relationship of C* vs. M_w holds true. Given that the Huggins and Kramer equations assume that the polymers do not aggregate in the solution state, the observed differences with experimental results is not surprising.[34]

The influence of solution concentration and polymer M_w on the hole mobility of DPP-DTT was investigated in **Figure 1d**. Notably, for each M_w, a peak hole mobility is obtained for OFET devices prepared from the solution concentrations near C*. This observation is in good agreement with our prior result where we hypothesized that the polymer chain overlap in the solution state at a concentration of C* appears to contribute to improved charge transport in the solid state.[30] For all three DPP-DTT samples, hole mobility decreased at solution concentrations greater than C*. It is likely that above C*, excessive chain interactions in the solid state lead to spatial defects or charge traps in the thin films.[15] Higher viscosity solutions were also observed to coat less uniform films, a feature that could also negatively impact performance. An almost identical trend was observed by Sarkar et al as they investigated the influence of film thickness on the device performance of OFETs fabricated from DPP-DTT using spin-coating and the thickness of the films was varied by tuning the solution concentration and spin rate.[31] Furthermore, the peak hole mobility decreases as M_w decreases: higher polymer M_w typically results in improved charge transport as a result of longer polymer chains that connect ordered domains[6, 7]. A similar trend was

observed for the OFET hole mobilities extracted from the forward transfer curve as shown in **Figure S4**. *These results indicate that there exists an optimum solution concentration, C*, for each of the M_w's investigated which can maximize charge transport as measured via OFET hole mobility.*

The respective transfer and output curves for the DPP-DTT devices studied here are presented in **Figures S5-S7** and **Figures S8-S10**, respectively. The transfer curves for the high M_w 290 kg/mol DPP-DTT show deviation from ideal behavior (hysteresis and different slope regions). The hysteresis is likely attributed to the degradation of the current during the measurement due to charge trapping occurring in the organic semiconductor or at the interface.[4] In addition to hysteresis, two regions of different slopes at the lower and higher voltages were observed. This behavior can lead to mobility overestimation - a phenomenon that has been observed for other D-A polymer systems,[7, 12, 47, 48] and is typically attributed to large contact resistance because of a large injection barrier at the contacts.[3, 4, 49] Hence, the linear region with a lower slope (higher V_g) was used to extract a more conservative estimate for hole mobility that is closer to the representative value. These deviations from ideal behavior were significantly reduced for the lower M_w DPP-DTT polymers (204 kg/mol, 110 kg/mol). Although the peak hole mobility decreased, there was a reduction in hysteresis and two-regime behavior was not apparent. Thus, consideration should be given to lower M_w D-A polymers to avoid deviations from ideal transfer curve behavior, even if hole mobility may be somewhat compromised. The average threshold voltage (V_{th}) and I_{on}/I_{off} extracted from the transfer curves for the three different M_w polymers as a function of solution concentration are given in **Figure S11** where it can be observed that all three DPP-DTT samples investigated here exhibit an increase in V_{th} as a function of solution concentration with no obvious trend for I_{on}/I_{off}.

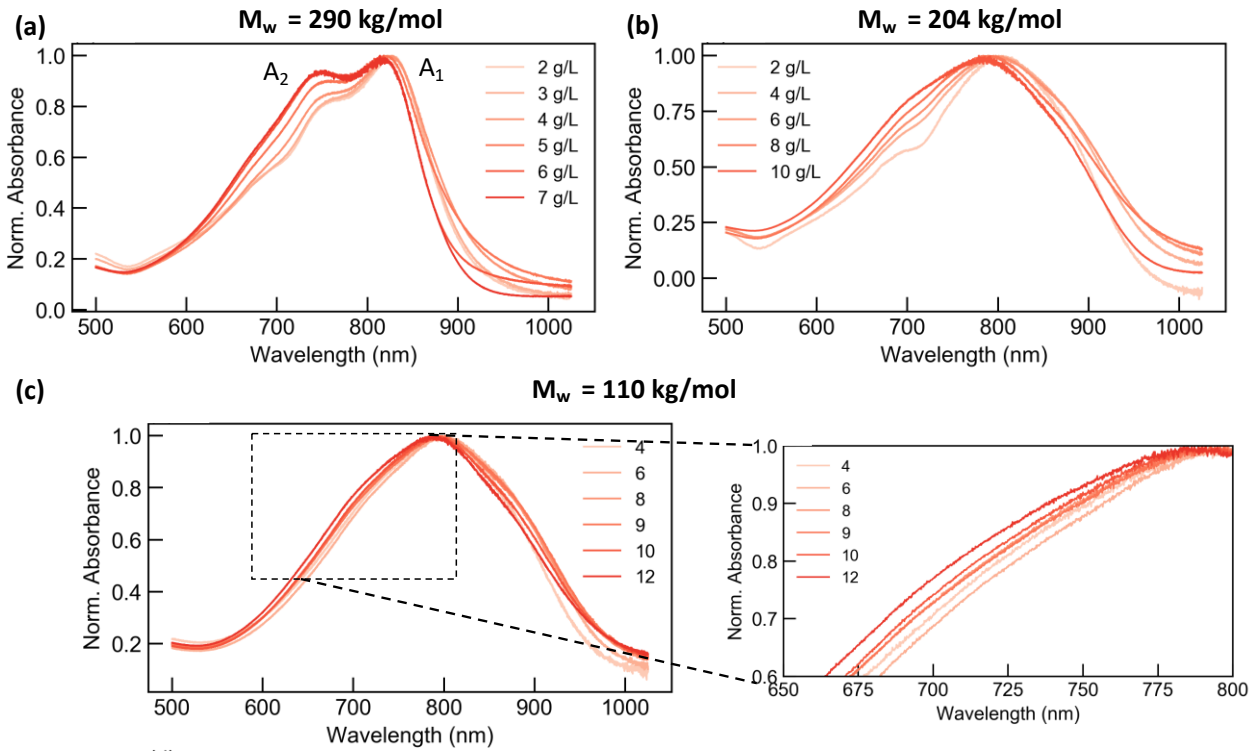

Figure 2. Normalized UV-Vis linear absorption spectra of DPP-DTT thin films prepared from the range of solution concentrations investigated respectively for three different weight average molecular weights (a) 290 kg/mol, (b) 204 kg/mol and (c) 110 kg/mol.

UV-Vis absorption spectroscopy was used to probe the influence of solution concentration on the solid-state polymer chain excitonic interactions for the three different M_w's of DPP-DTT as shown in **Figure 2**, with a focus on the absorption band in the low energy range that is assigned to the π-π* transition of the DPP unit.[31, 50, 51] For all three DPP-DTT samples, an increase in the intensity of the spectra in the ~750 nm region with increasing solution concentration can be observed, along with a blueshift which indicates increased excitonic interchain interactions. Such behavior corresponds to the H-type aggregation, as previously seen in spin-coated P3HT thin films, where the chromophores have a side-by-side geometry, leading to an increased excited state energy.[52, 53] For the high M_w DPP-DTT (290 kg/mol) in **Figure 2a**, two peaks can be observed at ~820 and 750 nm that are assigned to the A_1 and A_2 peaks of the vibronic transitions of the DPP π-π* transition, respectively. The ratio of the vibronic progressions of the A_1 and A_2 peak and the exciton bandwidth, extracted using the modified Franck-Condon analysis given in **Figure S12**, provides information on the packing order of the photophysical aggregates as a function of solution concentration. Normally, a lower ratio of the A_1 and A_2 peak, thus larger exciton bandwidth, W, indicates more enhanced interchain Coulombic interactions and/or reduced intrachain excitonic

interactions.[54] Therefore, the decreasing trend for A_1/A_2 with increasing solution concentration suggests that films coated at semi-dilute concentrations (>C*) may adopt more H-aggregate configurations as compared to films prepared from dilute solutions (<C*). For the two lower M_w polymers (204 and 110 kg/mol), a distinctive A_2 peak is no longer observed; rather, the peak becomes broader especially for films prepared from higher solution concentrations. This spectral behavior could be due to the formation of more disordered photophysical aggregates, and the inhomogeneous broadening hides the pronounced vibronic structure. Note that polymorphs have been observed, especially in low molecular weight DPP-based polymers M_w's.[50, 51, 55-57] The featureless spectral line shapes could originate from the overall absorption of the different aggregates in each polymorph. Nevertheless, the two major vibronic peaks at around 700 and 800 nm can be still ascribed to the absorption of the aggregate in the dominant polymorph as seen in the highest M_w DPP-DTT. The decrease in the A_1/A_2 ratio along with the blue-shift with increasing solution concentration observed for all three Mw's of DPP-DTT verifies that films prepared from higher solution concentrations lead to more H-type aggregation. Recently, Zheng, et al. further investigated the influence of solution concentration on the excitonic interactions and chain conformation of DPP-DTT using additional photophysical techniques including photoluminescence, transient absorption and resonance Raman spectroscopy supported by *ab initio* calculations.[58] Results revealed that an increase in the solution concentration resulted in the exciton being more dispersed along the polymer chain backbone, indicating that polymer chain order is enhanced when DPP-DTT is processed at higher concentrations.

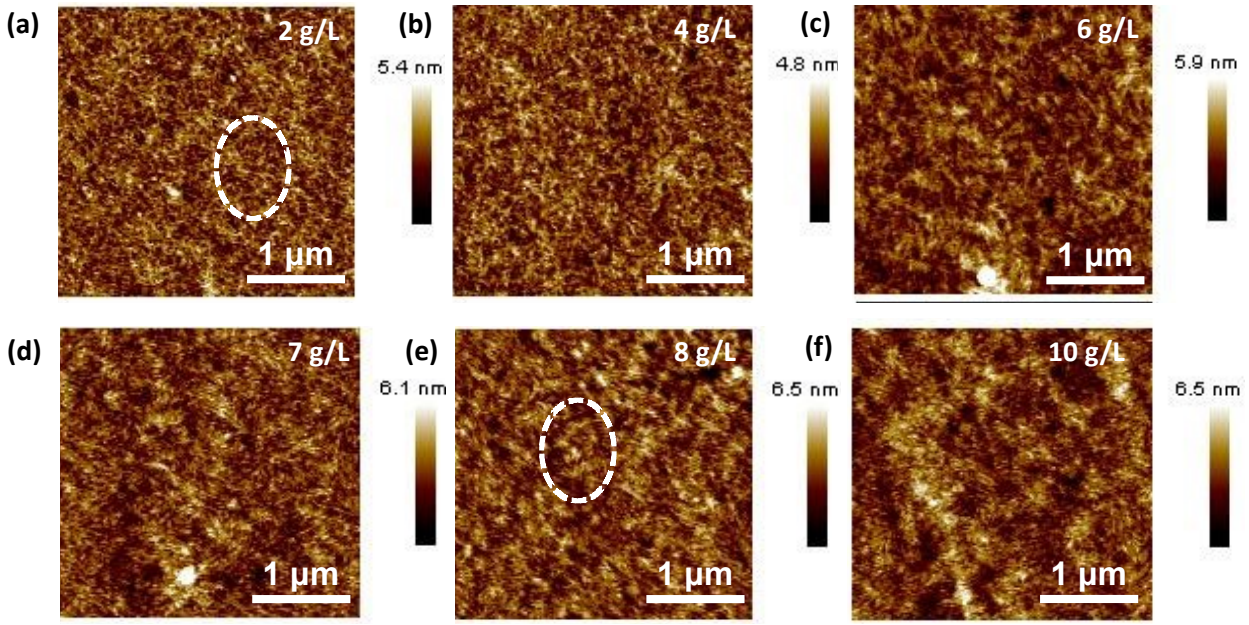

Figure 3. Atomic Force Microscopy height images of DPP-DTT (M_w = 204 kg/mol) thin films prepared from the range of solution concentrations (2-10 g/L) investigated. Thin films prepared from semi-dilute concentrations (> C) exhibit coarser domains that and appear more self-ordered as compared to films prepared from dilute concentrations.*

The influence of solution concentration on the surface morphology of the DPP-DTT thin films was investigated using AFM and the height images are provided in **Figure 3** for M_w of 204 kg/mol and **Figures S13 and 14** for M_w of 290 and 110 kg/mol, respectively. For all three Mw's investigated here, it can be observed that as the solution concentration increases, there is a shift in the thin-film morphology with a transition in behavior occurring near C*. Films prepared at semi-dilute concentrations (> C*) display relatively coarser domains that overlap and appear more self-ordered, while films prepared at dilute concentrations (<C*) display fine-grained domains with apparently less self-organization. This can be further supported by the observed increasing surface roughness of films fabricated from higher concentrations as shown in **Tables S2-4**. In addition to AFM, the cross-polarized optical microscopy (CPOM) images for the films prepared from different solution concentrations are shown in **Figures S15-17.** CPOM results reveal relatively smooth films for the range of concentrations investigated, with no obvious ordered structures observed at the length scale investigated and no birefringence. The thickness of the DPP-DTT films prepared from varying solution concentrations for the samples are presented in **Figure S18**. As expected, the film thickness increases with increasing solution concentration, suggesting that the films were fabricated in the evaporation regime.[23, 24]

GIWAXS measurements were conducted on thin films of 290 kg/mol DPP-DTT to explore microstructural transitions and changes in the molecular packing in the films as a function of solution concentration. Examination of the 2-dimensional GIWAXS patterns provided in **Figure S19** shows that most of the films possess an 'edge-on' orientation with respect to the substrate. **Figure S20** shows the out-of-plane and in-plane scattering signals. An increase in the intensity of the scattering signal with increasing solution concentration was observed for both the out-of-plane and in-plane cases, which may imply an increase in the aggregation within the films prepared from higher solution concentrations. The GIWAXS results are in agreement with AFM and UV-Vis observations.[17, 31, 50] The lamellar and π-π spacing, coherence length, full width half maximum and paracrystallinity (g) values extracted from the out-of-plane and in-plane scattering signals are given in **Table S2**. No significant changes in lamellar and π-π spacing values as a function of solution concentration were observed, suggesting that the solution concentration does not impact molecular packing within the film. Lamellar spacing (100) and π-π spacing (010) values were ~19.6 and ~3.7 Å, respectively, which are in good agreement with the reported values.[17, 31, 50]

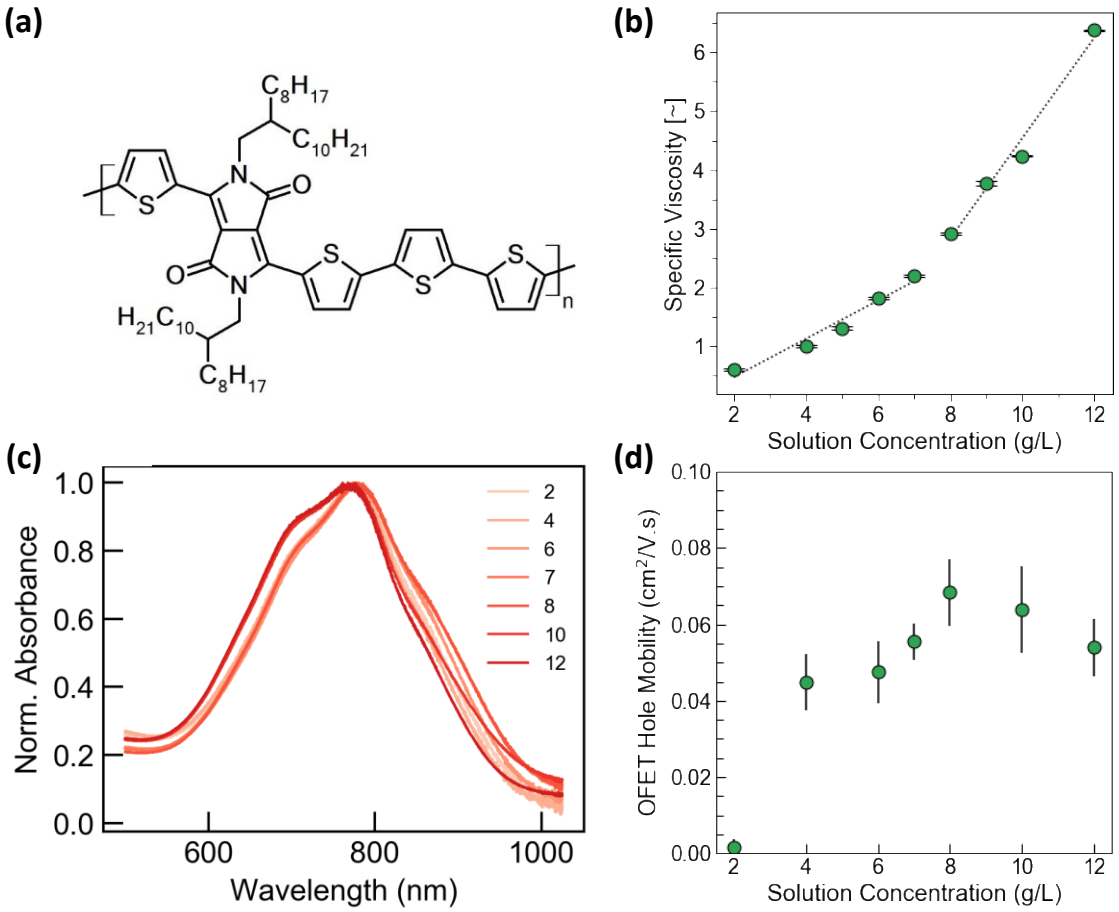

Figure 4. (a) Schematic of molecular structure of PDPP-4T (M_w = 75 kg/mol). (b) Specific viscosity measurement of PDPP-4T dissolved in chlorobenzene solutions at 56 °C. The error bars represent the standard deviation of the specific viscosity. The C extracted from the plot is 8 g/L (c) Normalized UV-Vis linear absorption spectra of PDPP-4T thin films prepared from solution concentrations ranging from 2 to 12 g/L. (d) FET hole mobility of PDPP-4T thin films extracted from the backward sweep Transfer Curve (V_{DS} = -80V) as a function of solution concentration. The error bars here represent 95% confidence intervals averaged over 18 OFET devices.*

In addition to investigating the influence of solution concentration on different molecular weights of DPP-DTT, an alternative DPP based polymer, namely PDPP-4T (**Figure 4a**), was examined with 2–12 g/L solutions in chlorobenzene. The solution state viscosity results revealed a similar two regime behavior with the C* occurring at 8 g/L as shown in **Figure 4b**. Further, OFETs prepared from the range of solution concentrations studied revealed a peak hole mobility at the C* of 8 g/L, followed by a decrease in the average hole mobility at semi-dilute concentrations. *This result indicates that the trend observed previously with DPP-DTT may be generalizable across different DPP based polymers*. In the case of PDPP-4T, the UV-Vis absorption spectra exhibit two distinctive peaks observed at ~720 nm and 775 nm. Although the shape of the spectra differs slightly from DPP-DTT, a similar increase in the intensity of the peak at ~720 nm along with a blue shift with increasing solution concentration is observed. Thus, solution concentration likely

influences polymer chain excitonic interactions for not just DPP-DTT but other DPP-based polymers as well. The PDPP-4T transfer curves, output curves, and extracted device parameters (V_{th} and $I_{on/off}$) as a function of solution concentration are shown in **Figure S21-23** respectively. Lastly, the PDPP-4T thin-film AFM and CPOM images (**Figure S24 and S25**) reveal a similar trend to that observed for DPP-DTT, with films prepared from semi-dilute concentrations showing mostly self-ordered and overlapped domains as compared to films prepared from dilute concentrations.

Conclusions

In this work, we investigated the influence of solution concentration on the final thin-film morphology and device performance of D-A polymers, with a focus on DPP-based copolymers. DPP-DTT, at three significantly different M_w's, was selected as a model for other DPP based D-A polymer candidates. Viscosity results revealed that an overlap concentration, C*, existed for all three M_w's of DPP-DTT investigated, with the C* scaling inversely with M_w. Notably, OFET devices prepared from a solution concentration of C* displayed improved hole mobilities irrespective of the M_w, although the improvement at C* was most pronounced at the highest M_w explored. UV-Vis spectroscopic interrogation revealed that films prepared at semi-dilute concentrations are more aggregated and display more interchain interaction than at dilute concentrations, while AFM imaging revealed that films prepared from dilute concentrations (<C*) displayed a lack of aggregates and mostly fine-grained domains with less self-organization. For films prepared from concentrations approaching C*, increased aggregation was observed, with the formation of coarser domains that overlap and become more ordered at increasing solution concentrations. These results were confirmed through GIWAXS studies demonstrating that films prepared from higher solution concentrations displayed increased aggregation. Significantly, a similar correlation between solution concentration and device performance was observed with an alternative DPP-based polymer, PDPP-4T, further strengthening our findings.

This work further highlights the importance of probing the solution state of conjugated polymers prior to deposition in order to control the final thin film morphology and improve device performance. Our findings highlight that polymer solution concentration is an important processing parameter linked to macroscale device performance of D-A polymers and there exists

an optimum solution concentration that results in improved charge transport, C*, which can be obtained from relatively straightforward viscometry experiments. This study also opens up questions about how the solution concentration influences the polymer chain conformations and aggregation in the solution state. In addition to the viscosity experiments, more comprehensive techniques such as DFT calculations and/or MD simulations in tandem with SANS/SAXS experiments would help obtain a better understanding of the influence of the parameter on the solution phase behavior of D-A polymers and the transition to the final film state.

ASSOCIATED CONTENT

Supporting Information

The supporting information is available free of charge at:

AUTHOR INFORMATION

Corresponding Authors

Carson Meredith – School of Chemical & Biomolecular Engineering, Georgia Institute of Technology, 311 Ferst Drive, Atlanta, GA, 30332. Email: carson.meredith@chbe.gatech.edu

Martha A. Grover – School of Chemical & Biomolecular Engineering, Georgia Institute of Technology, 311 Ferst Drive, Atlanta, GA, 30332. Email: martha.grover@chbe.gatech.edu

Elsa Reichmanis – Department of Chemical & Biomolecular Engineering, Lehigh University, 124 E. Morton Street, Bethlehem, PA 18015. Email: elr420@lehigh.edu

Other Authors

Aaron L. Liu - School of Chemical & Biomolecular Engineering, Georgia Institute of Technology, 311 Ferst Drive, Atlanta, GA, 30332;

Carlos Silva - School of Chemistry and Biochemistry, Georgia Institute of Technology, 908 Atlantic Drive, Atlanta, GA, 30332; School of Physics, Georgia Institute of Technology, Atlanta, GA 30332

Christopher J. Takacs - Stanford Synchrotron Radiation Light Source, SLAC National Accelerator Laboratory, Menlo Park, CA, 94025

Haoqun Zhao – School of Chemical & Biomolecular Engineering, Georgia Institute of Technology, 311 Ferst Drive, Atlanta, GA, 30332

Rahul Venkatesh – School of Chemical & Biomolecular Engineering, Georgia Institute of Technology, 311 Ferst Drive, Atlanta, GA, 30332

Yulong Zheng – School of Chemistry and Biochemistry, Georgia Institute of Technology, 801 Atlantic Drive, Atlanta, GA, 30332

ORCID:
Elsa Reichmanis: 0000-0002-8205-8016
Martha Grover: 0000-0002-7036-776X
Carson Meredith: 0000-0003-2519-5003

Carlos Silva: 0000-0002-3969-5271
Rahul Venkatesh: 0000-0003-1008-6568
Yulong Zheng: 0000-0001-5136-1971
Aaron L. Liu: 0000-0001-7347-5347
Haoqun Zhao: 0000-0002-3871-0302
Christopher J. Takacs: 0000-0001-9126-6901

Notes
The authors declare no conflict of interest.

Acknowledgments

The authors would like to acknowledge the National Science Foundation Grant No. 1922111, DMREF: Collaborative Research: Achieving Multicomponent Active Materials through Synergistic Combinatorial, Informatics-enabled Materials Discovery for support. This work was performed in part at the Georgia Tech Institute for Electronics and Nanotechnology, a member of the National Nanotechnology Coordinated Infrastructure (NNCI), which is supported by the National Science Foundation (ECCS-2025462); E.R. appreciates support associated with Carl Robert Anderson Chair funds at Lehigh University. Use of the Stanford Synchrotron Radiation Lightsource, SLAC National Accelerator Laboratory, is supported by the U.S. Department of Energy, Office of Science, Office of Basic Energy Sciences under Contract No. DE-AC02-76SF00515. The authors also appreciate discussions with Paul Russo and Marlow Dublin regarding viscometry and access to viscometric characterization tools available in the Open Polymer Active Learning Laboratory (OPALL) and Marlow Dublin regarding solution-state polymer conformations at Georgia Tech.

References

1. Sekine, C.; Tsubata, Y.; Yamada, T.; Kitano, M.; Doi, S., Recent Progress of High Performance Polymer OLED and OPV Materials for Organic Printed Electronics. *Science and Technology of Advanced Materials* **2014,** *15* (3), 34203-34218.
2. Facchetti, A., π-Conjugated Polymers for Organic Electronics and Photovoltaic Cell Applications. *Chemistry of Materials* **2011,** *23* (3), 733-758.
3. Lamport, Z. A.; Haneef, H. F.; Anand, S.; Waldrip, M.; Jurchescu, O. D., Tutorial: Organic field-effect transistors: Materials, structure and operation. *Journal of Applied Physics* **2018,** *124* (7), 071101.
4. Sirringhaus, H., 25th Anniversary Article: Organic Field-Effect Transistors: The Path Beyond Amorphous Silicon. *Advanced Materials* **2014,** *26* (9), 1319-1335.
5. Zhu, C.; Liu, L.; Yang, Q.; Lv, F.; Wang, S., Water-Soluble Conjugated Polymers for Imaging, Diagnosis, and Therapy. *Chemical Reviews* **2012,** *112* (8), 4687-4735.
6. Kim, M.; Ryu, S. U.; Park, S. A.; Choi, K.; Kim, T.; Chung, D.; Park, T., Donor–Acceptor-Conjugated Polymer for High-Performance Organic Field-Effect Transistors: A Progress Report. *Advanced Functional Materials* **2020,** *30* (20), 1904545.
7. Li, J.; Zhao, Y.; Tan, H. S.; Guo, Y.; Di, C.-A.; Yu, G.; Liu, Y.; Lin, M.; Lim, S. H.; Zhou, Y.; Su, H.; Ong, B. S., A stable solution-processed polymer semiconductor with record high-mobility for printed transistors. *Scientific Reports* **2012,** *2* (1), 754.
8. Arias, A. C.; MacKenzie, J. D.; McCulloch, I.; Rivnay, J.; Salleo, A., Materials and applications for large area electronics: solution-based approaches. *Chem Rev* **2010,** *110* (1), 3-24.
9. Haase, K.; Hambsch, M.; Teixeira da Rocha, C.; Zessin, J.; Mannsfeld, S. C. B., 17 - Advances in solution processing of organic materials for devices. In *Handbook of Organic Materials for Electronic and Photonic Devices (Second Edition)*, Ostroverkhova, O., Ed. Woodhead Publishing: 2019; pp 551-577.
10. Alkan, M.; Yavuz, I., Intrinsic charge-mobility in benzothieno[3,2-b][1]benzothiophene (BTBT) organic semiconductors is enhanced with long alkyl side-chains. *Physical Chemistry Chemical Physics* **2018,** *20* (23), 15970-15979.
11. Kang, B.; Kim, R.; Lee, S. B.; Kwon, S.-K.; Kim, Y.-H.; Cho, K., Side-Chain-Induced Rigid Backbone Organization of Polymer Semiconductors through Semifluoroalkyl Side Chains. *Journal of the American Chemical Society* **2016,** *138* (11), 3679-3686.
12. Kang, I.; An, T. K.; Hong, J.-a.; Yun, H.-J.; Kim, R.; Chung, D. S.; Park, C. E.; Kim, Y.-H.; Kwon, S.-K., Effect of Selenophene in a DPP Copolymer Incorporating a Vinyl Group for High-Performance Organic Field-Effect Transistors. *Advanced Materials* **2013,** *25* (4), 524-528.
13. Liu, J.; Ma, L.-K.; Li, Z.; Hu, H.; Sheong, F. K.; Zhang, G.; Ade, H.; Yan, H., Donor polymer based on alkylthiophene side chains for efficient non-fullerene organic solar cells: insights into fluorination and side chain effects on polymer aggregation and blend morphology. *Journal of Materials Chemistry A* **2018,** *6* (46), 23270-23277.
14. Liu, X.; He, B.; Garzón-Ruiz, A.; Navarro, A.; Chen, T. L.; Kolaczkowski, M. A.; Feng, S.; Zhang, L.; Anderson, C. A.; Chen, J.; Liu, Y., Unraveling the Main Chain and Side Chain Effects on Thin Film Morphology and Charge Transport in Quinoidal Conjugated Polymers. *Advanced Functional Materials* **2018,** *28* (31), 1801874.
15. Koch, F. P. V.; Rivnay, J.; Foster, S.; Müller, C.; Downing, J. M.; Buchaca-Domingo, E.; Westacott, P.; Yu, L.; Yuan, M.; Baklar, M.; Fei, Z.; Luscombe, C.; McLachlan, M. A.; Heeney, M.; Rumbles, G.; Silva, C.; Salleo, A.; Nelson, J.; Smith, P.; Stingelin, N., The

impact of molecular weight on microstructure and charge transport in semicrystalline polymer semiconductors–poly(3-hexylthiophene), a model study. *Progress in Polymer Science* **2013,** *38* (12), 1978-1989.
16. Boehm, B. J.; McNeill, C. R.; Huang, D. M., Competing single-chain folding and multi-chain aggregation pathways control solution-phase aggregate morphology of organic semiconducting polymers. *Nanoscale* **2022**.
17. Xi, Y.; Wolf, C. M.; Pozzo, L. D., Self-assembly of donor–acceptor conjugated polymers induced by miscible 'poor' solvents. *Soft Matter* **2019,** *15* (8), 1799-1812.
18. Xu, Z.; Park, K. S.; Kwok, J. J.; Lin, O.; Patel, B. B.; Kafle, P.; Davies, D. W.; Chen, Q.; Diao, Y., Not All Aggregates Are Made the Same: Distinct Structures of Solution Aggregates Drastically Modulate Assembly Pathways, Morphology, and Electronic Properties of Conjugated Polymers. *Advanced Materials* **2022,** *34* (32), 2203055.
19. Lei, Y.; Deng, P.; Li, J.; Lin, M.; Zhu, F.; Ng, T.-W.; Lee, C.-S.; Ong, B. S., Solution-Processed Donor-Acceptor Polymer Nanowire Network Semiconductors For High-Performance Field-Effect Transistors. *Scientific Reports* **2016,** *6* (1), 24476.
20. Pan, Y.; Yu, G., Multicomponent Blend Systems Used in Organic Field-Effect Transistors: Charge Transport Properties, Large-Area Preparation, and Functional Devices. *Chemistry of Materials* **2021,** *33* (7), 2229-2257.
21. Li, M.; Bin, H.; Jiao, X.; Wienk, M. M.; Yan, H.; Janssen, R. A. J., Controlling the Microstructure of Conjugated Polymers in High-Mobility Monolayer Transistors via the Dissolution Temperature. *Angewandte Chemie International Edition* **2020,** *59* (2), 846-852.
22. Singh, C.; Hone, D., Temperature-dependent behavior of conjugated polymers in solution. *Synthetic Metals* **1994,** *62* (1), 61-70.
23. Chen, M.; Peng, B.; Huang, S.; Chan, P. K. L., Understanding the Meniscus-Guided Coating Parameters in Organic Field-Effect-Transistor Fabrications. *Advanced Functional Materials* **2020,** *30* (1), 1905963.
24. Gu, X.; Shaw, L.; Gu, K.; Toney, M. F.; Bao, Z., The meniscus-guided deposition of semiconducting polymers. *Nature Communications* **2018,** *9* (1), 534.
25. Afzal, T.; Iqbal, M. J.; Iqbal, M. Z.; Sajjad, A.; Raza, M. A.; Riaz, S.; Kamran, M. A.; Numan, A.; Naseem, S., Effect of post-deposition annealing temperature on the charge carrier mobility and morphology of DPPDTT based organic field effect transistors. *Chemical Physics Letters* **2020,** *750*, 137507.
26. Holliday, S.; Donaghey, J. E.; McCulloch, I., Advances in Charge Carrier Mobilities of Semiconducting Polymers Used in Organic Transistors. *Chemistry of Materials* **2014,** *26* (1), 647-663.
27. Callaway, C. P.; Liu, A. L.; Venkatesh, R.; Zheng, Y.; Lee, M.; Meredith, J. C.; Grover, M.; Risko, C.; Reichmanis, E., The Solution is the Solution: Data-Driven Elucidation of Solution-to-Device Feature Transfer for π-Conjugated Polymer Semiconductors. *ACS Applied Materials & Interfaces* **2022,** *14* (3), 3613-3620.
28. Kwok, J. J.; Park, K. S.; Patel, B. B.; Dilmurat, R.; Beljonne, D.; Zuo, X.; Lee, B.; Diao, Y., Understanding Solution State Conformation and Aggregate Structure of Conjugated Polymers via Small Angle X-ray Scattering. *Macromolecules* **2022,** *55* (11), 4353-4366.
29. Xu, Z.; Park, K. S.; Diao, Y., What Is the Assembly Pathway of a Conjugated Polymer From Solution to Thin Films? *Frontiers in Chemistry* **2020,** *8*.

30. Venkatesh, R.; Zheng, Y.; Viersen, C.; Liu, A.; Silva, C.; Grover, M.; Reichmanis, E., Data Science Guided Experiments Identify Conjugated Polymer Solution Concentration as a Key Parameter in Device Performance. *ACS Materials Letters* **2021,** *3* (9), 1321-1327.
31. Sarkar, T.; Schneider, S. A.; Ankonina, G.; Hendsbee, A. D.; Li, Y.; Toney, M. F.; Frey, G. L., Tuning Intra and Intermolecular Interactions for Balanced Hole and Electron Transport in Semiconducting Polymers. *Chemistry of Materials* **2020,** *32* (17), 7338-7346.
32. Yao, Z.-F.; Zheng, Y.-Q.; Li, Q.-Y.; Lei, T.; Zhang, S.; Zou, L.; Liu, H.-Y.; Dou, J.-H.; Lu, Y.; Wang, J.-Y.; Gu, X.; Pei, J., Wafer-Scale Fabrication of High-Performance n-Type Polymer Monolayer Transistors Using a Multi-Level Self-Assembly Strategy. *Advanced Materials* **2019,** *31* (7), 1806747.
33. Rubinstein, M.; Colby, R., *Polymer Physics*. Oxford University Press: 2003.
34. Sperling, L. H., *Introduction to Physical Polymer Science*. 4 ed.; Wiley: 2005.
35. Zierenberg, J.; Marenz, M.; Janke, W., Dilute Semiflexible Polymers with Attraction: Collapse, Folding and Aggregation. *Polymers* **2016,** *8* (9), 333.
36. Kuei, B.; Gomez, E. D., Chain conformations and phase behavior of conjugated polymers. *Soft Matter* **2017,** *13* (1), 49-67.
37. Hu, H.; Zhao, K.; Fernandes, N.; Boufflet, P.; Bannock, J. H.; Yu, L.; de Mello, J. C.; Stingelin, N.; Heeney, M.; Giannelis, E. P.; Amassian, A., Entanglements in marginal solutions: a means of tuning pre-aggregation of conjugated polymers with positive implications for charge transport. *Journal of Materials Chemistry C* **2015,** *3* (28), 7394-7404.
38. Lopes, L.; Silveira, B. M.; Moreno, R. B. Z. L. In *Rheological Evaluation of HPAM fluids for EOR Applications*, 2014.
39. Maron, S. H.; Nakajima, N.; Krieger, I. M., Study of entanglement of polymers in solution by viscosity measurements. *Journal of Polymer Science* **1959,** *37* (131), 1-18.
40. Pierri, E.; Papanagopoulos, D.; Dondos, A., The influence of shear rate, temperature and chain conformation on the critical concentration c. *Colloid and Polymer Science* **1997,** *275* (8), 709-715.
41. Porter, R. S.; Johnson, J. F., The Entanglement Concept in Polymer Systems. *Chemical Reviews* **1966,** *66*, 1-27.
42. Wang, P.-S.; Lu, H.-H.; Liu, C.-Y.; Chen, S.-A., Gel Formation via Physical Cross-Linking in the Soluble Conjugated Polymer, Poly[2-methoxy-5-(2-ethylhexyloxy)-1,4-phenylenevinylene], in Solution by Addition of Alkanes. *Macromolecules* **2008,** *41* (17), 6500-6504.
43. Gupta, P.; Elkins, C.; Long, T. E.; Wilkes, G. L., Electrospinning of linear homopolymers of poly(methyl methacrylate): exploring relationships between fiber formation, viscosity, molecular weight and concentration in a good solvent. *Polymer* **2005,** *46* (13), 4799-4810.
44. Lopez, C. G.; Richtering, W., Viscosity of Semidilute and Concentrated Nonentangled Flexible Polyelectrolytes in Salt-Free Solution. *The Journal of Physical Chemistry B* **2019,** *123* (26), 5626-5634.
45. Shenoy, S. L.; Bates, W. D.; Frisch, H. L.; Wnek, G. E., Role of chain entanglements on fiber formation during electrospinning of polymer solutions: good solvent, non-specific polymer–polymer interaction limit. *Polymer* **2005,** *46* (10), 3372-3384.
46. Masuelli, M. A., Intrinsic Viscosity Determination of High Molecular Weight Biopolymers by Different Plot Methods. Chia Gum Case. *Journal of Polymer and Biopolymer Physics Chemistry* **2018,** *6* (1), 13-25.

47. Chen, H.; Guo, Y.; Yu, G.; Zhao, Y.; Zhang, J.; Gao, D.; Liu, H.; Liu, Y., Highly π-extended copolymers with diketopyrrolopyrrole moieties for high-performance field-effect transistors. *Adv Mater* **2012,** *24* (34), 4618-22.
48. Lei, T.; Dou, J.-H.; Pei, J., Influence of Alkyl Chain Branching Positions on the Hole Mobilities of Polymer Thin-Film Transistors. *Advanced Materials* **2012,** *24* (48), 6457-6461.
49. McCulloch, I.; Salleo, A.; Chabinyc, M., Avoid The Kinks when Measuring Mobility. *Science* **2016,** *352* (6293), 1521.
50. Chen, Z.; Lee, M. J.; Shahid Ashraf, R.; Gu, Y.; Albert-Seifried, S.; Meedom Nielsen, M.; Schroeder, B.; Anthopoulos, T. D.; Heeney, M.; McCulloch, I.; Sirringhaus, H., High-performance ambipolar diketopyrrolopyrrole-thieno[3,2-b]thiophene copolymer field-effect transistors with balanced hole and electron mobilities. *Adv Mater* **2012,** *24* (5), 647-52.
51. Li, M.; Balawi, A. H.; Leenaers, P. J.; Ning, L.; Heintges, G. H. L.; Marszalek, T.; Pisula, W.; Wienk, M. M.; Meskers, S. C. J.; Yi, Y.; Laquai, F.; Janssen, R. A. J., Impact of polymorphism on the optoelectronic properties of a low-bandgap semiconducting polymer. *Nat Commun* **2019,** *10* (1), 2867.
52. Clark, J.; Chang, J.-F.; Spano, F. C.; Friend, R. H.; Silva, C., Determining Exciton Bandwidth and Film Microstructure in Polythiophene Films using Linear Absorption Spectroscopy. *Applied Physics Letters* **2009,** *94* (16), 163306-163311.
53. Spano, F. C., Absorption in regio-regular poly(3-hexyl)thiophene thin films: Fermi resonances, interband coupling and disorder. *Chemical Physics* **2006,** *325* (1), 22-35.
54. Qarai, M. B.; Chang, X.; Spano, F. C., Vibronic exciton model for low bandgap donor–acceptor polymers. *The Journal of Chemical Physics* **2020,** *153* (24), 244901-1:16.
55. Armin, A.; Wolfer, P.; Shaw, P. E.; Hambsch, M.; Maasoumi, F.; Ullah, M.; Gann, E.; McNeill, C. R.; Li, J.; Shi, Z.; Burn, P. L.; Meredith, P., Simultaneous enhancement of charge generation quantum yield and carrier transport in organic solar cells. *Journal of Materials Chemistry C* **2015,** *3* (41), 10799-10812.
56. Lin, H.-W.; Lee, W.-Y.; Chen, W.-C., Selenophene-DPP donor–acceptor conjugated polymer for high performance ambipolar field effect transistor and nonvolatile memory applications. *Journal of Materials Chemistry* **2012,** *22* (5), 2120-2128.
57. Yun, H.-J.; Kang, S.-J.; Xu, Y.; Kim, S. O.; Kim, Y.-H.; Noh, Y.-Y.; Kwon, S.-K., Dramatic Inversion of Charge Polarity in Diketopyrrolopyrrole-Based Organic Field-Effect Transistors via a Simple Nitrile Group Substitution. *Advanced Materials* **2014,** *26* (43), 7300-7307.
58. Zheng, Y.; Venkatesh, R.; Callaway, C. P.; Viersen, C.; Fagbohungbe, K. H.; Liu, A.; Takacs, C. J.; Risko, C.; Reichmanis, E.; Silva-Acuna, C., Exciton delocalization and chain conformation in a push-pull conjugated polymer. *To be submitted* **2023**.